

DEVELOPMENT AND TESTING OF CARBON-BASED ION OPTICS FOR 30-CM ION THRUSTERS

John Steven Snyder,^{*} John R. Brophy,[†] Dan M. Goebel,[†] and John S. Beatty[‡]

*Jet Propulsion Laboratory
California Institute of Technology
Pasadena, CA 91109*

*Michael K. De Pano^{**}
Boeing Electron Dynamic Devices, Inc.
Torrance, CA 90509*

Carbon-based ion optics have the potential to significantly increase the lifetime of state-of-the-art ion thrusters which use molybdenum optics because of the lower sputter yield and greater packing density of the carbon materials. There are issues associated with the use of carbon grids, however, which must be addressed: manufacturing and process control, launch survivability, and voltage standoff. The Jet Propulsion Laboratory and Boeing Electron Dynamic Devices, Inc., are addressing each of these issues in the Carbon-Based Ion Optics (CBIO) program. Thirty-centimeter optics manufactured from both carbon-carbon (CC) and pyrolytic graphite (PG) have been designed to operate at a specific impulse of 4000 sec while maximizing the mechanical robustness and minimizing the intra-grid electric field. Grid fabrication and process control methods while enable this design are described. These methods are shown to produce significantly better-controlled CC grids than previous generations of grids. Dished 30-cm CC grids were successfully vibration tested at levels up to 18.6 Grms and the test results are shown to be within several percent of model predictions. The voltage stand-off capability of CC and PG materials have been characterized and it is shown that arc damage to CC surfaces can be suppressed by limiting the total coulomb transfer during an arc event. Differential sputter yield data are being obtained for use in lifetime modeling of carbon-based grids; yields for PG at 1-keV xenon ion energies are presented. Finally, an earlier-generation flat 30-cm CC grid set was operated at Isp's of up to 5300 sec and optics performance measurements are presented.

INTRODUCTION

Carbon grid technology for ion thrusters has been under investigation for over a decade by many different laboratories. Most of this work has been done with carbon-carbon composite materials at JPL,¹⁻³ Boeing,⁴ and in Japan.⁵⁻⁸ Laboratory results have been encouraging and have led to the use of carbon-carbon technology on the MUSES-C spacecraft,⁵ launched recently and now in operation. Recently, NASA Glenn Research Center has successfully fabricated and tested pyrolytic graphite grids.⁹

^{*} Member of the Technical Staff, Advanced Propulsion Technology Group, Member AIAA

[†] Section Staff, Thermal and Propulsion Engineering Section, Member AIAA

[‡] Composite Engineer, Materials Testing and Contamination Control Group

^{**} Member of the Technical Staff, Electric Propulsion Product Line, Member AIAA

Carbon-based materials are attractive for thruster grids largely because of their low sputter yields compared to molybdenum, which has been used on the majority of flight thrusters. For example, the service life of the NASA Solar Electric Propulsion Technology Applications Readiness (NSTAR) ion thruster at full power is limited by erosion of the molybdenum accelerator grid.¹⁰ Implementation of a carbon grid material that is more resistant to erosion could thus directly extend the thruster life and even possibly eliminate accelerator grid erosion as the primary life-limiting phenomenon of the thruster. Alternatively, carbon grids could permit higher-power thruster operation for a similar service life as the current molybdenum grids.

Carbon-based grids have been shown to produce similar performance as molybdenum grids,^{3,4,9} but there are also serious issues with the use of this material that must be addressed. Much of the research work performed to-date has shown that a comprehensive understanding and improvement of three major areas is necessary before carbon-based grids can be reliably implemented for space missions.

The first and most fundamental of those issues is manufacturability and process control. For example, grids fabricated from carbon-carbon materials have been shown to have poor dimensional control,¹ warped,^{4,8} delaminated,² and have been difficult to machine.³ Another important issue is the ability of the grids to survive launch loads. At least one vibration test of carbon-carbon grids has resulted in grid fracture. Finally, the grids must be able to stand off the required intra-grid electric fields for the lifetime of the thruster. Voltage standoff problems,⁷ arcing that causes localized damage to the grids,⁸ and damage that prevents the grids from being operated⁶ have been observed.

The Jet Propulsion Laboratory and Boeing Electron Dynamic Devices, Inc. (EDD) are now working on the Carbon-Based Ion Optics (CBIO) program to develop carbon grid technology, funded by the NASA Marshall Space Flight Center through the In-Space Transportation program. This program aims to bring carbon-based grids to a technology readiness level at which a qualification program may be initiated. Additionally, the present work described in this paper directly addresses each of the three major issues detailed in the preceding paragraph. It will be shown that each is a tractable problem and that solutions are being found.

CBIO Program Requirements

The overall objective of the CBIO program is to develop carbon grids for the 40-cm NASA Evolutionary Xenon Thruster¹¹ (NEXT) that will operate at a nominal Isp of 4000 sec. The program is separated into two phases. The Phase I effort focuses on the development and test of 30-cm carbon grids for operation on NSTAR-like thrusters. The objective of the Phase I effort is to: develop 30-cm carbon grids; validate the performance and life of carbon grids; develop grid life modeling software; and evaluate the feasibility of 40-cm carbon grid development. In Phase II, 40-cm-dia. carbon grids will be designed and fabricated for performance, vibration, and endurance

tests on the NEXT thruster. This paper describes work that has been performed to-date on Phase I.

Two forms of carbon grids are being investigated for Phase I: carbon-carbon composite (CC) led by JPL, and pyrolytic graphite (PG) led by Boeing EDD. The grid development occurs in two parallel paths with the two technologies in order to mitigate overall program risk. The CBIO team has full access to the data gathered from each institution to foster discussion and technology transfer with the ultimate goal of learning as much about carbon-based ion optics for use in long life ion thrusters as the program allows.

The performance design requirements that the optics must meet were derived from the NEXT requirements and scaled to the NSTAR thruster. Both types of carbon grids must meet the requirements for screen grid transparency, perveance margin, and electron backstreaming margin at the operating conditions shown in Table 1. Each grid type will be vibration tested to NSTAR vibration levels and performance measurements will be made before and after the vibration testing. Vibration test data will be correlated with dynamic models to develop predictions of the responses of other grid designs to vibration loads. After completion of the performance and vibration testing a review will be held to determine which grid technology should be used for a 2000-hour endurance test to validate grid life models.

The grid life modeling is complicated by the lack of understanding of sputtering behavior of both PG and CC. Published sputter yields for CC have a significant amount of scatter as seen in Fig. 1. Some of the discrepancy is likely due to materials and surface topography differences which are known to affect sputter yields. Part of the CBIO effort thus includes accurate measurements of differential sputter yields of the PG and CC grid materials.

The final activities of Phase I are to evaluate the feasibility of fabricating 40-cm carbon grids for the NEXT thruster, and to propose for Phase II a development program of 40-cm grids fabricated for the NEXT thruster.

Table 1. Carbon Grid Performance Requirements.

Operating Point	Beam Current J_B (A)	Beam Voltage V_B (V)	Screen Grid Transparency	Margins	
				Perveance (V)	Electron Backstreaming (V)
1	1.76	1800	0.75	500	100
2	1.76	1400	0.60	100	100
3	1.01	1800	0.75	700	100
4	1.01	1200	0.60	100	100
5	0.75	1800	0.75	800	100
6	0.75	1100	0.60	100	100
7	0.34	1800	0.75	1200	100
8	0.34	679	0.60	100	100

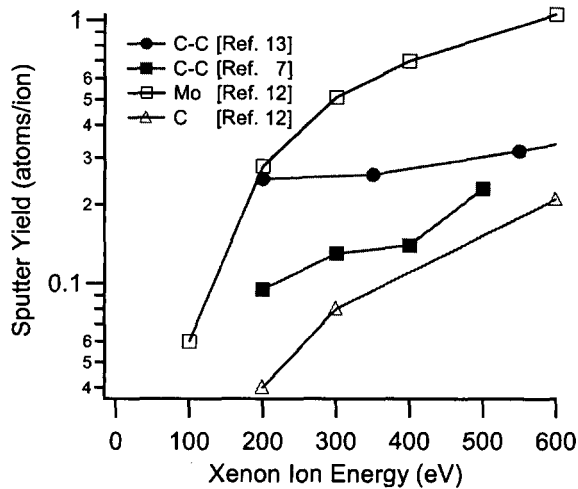


Fig. 1. Comparison of Sputter Yields for Thruster Grid Materials.

Several JPL activities for CBIO address the key challenges in using CC grids. Those challenges include developing designs that will survive vibration testing and yield the desired performance, achieving the design dimensions during grid fabrication, and electric field breakdown considerations and their impact on performance. These challenges are addressed by:

- Detailed process control during fabrication,
- Utilization of previous lessons learned in fabricating CC grids,
- Mechanical modeling of grids to validate vibration expectations,
- Ion optics design using 2D and 3D computer codes and a genetic search algorithm to determine the minimum acceptable electric field,
- Performance testing of existing CC grids to map out the operational limits and validate the computer codes, and
- Use of CC test coupons to investigate the effect of arc damage on sustainable electric field and determine beam power supply specifications to minimize arc damage.

DESIGN AND FABRICATION ACTIVITIES

Optics Design

The carbon grid design must meet the requirements for perveance margin, electron-backstreaming margin, and screen grid transparency over the full throttle envelope while maximizing the mechanical robustness of the screen grid and minimizing the intra-grid electric field. In addition, the grids must exhibit a substantial

improvement in grid life relative to the state-of-the-art molybdenum grids.

To meet the performance requirements listed in Table 1 four different ion optics geometries are being pursued. Three different CC grid geometries and one PG grid design are being fabricated. The first CC grid design and the PG design attempt to reproduce the NSTAR ion optics geometry as closely as possible. For the CC grids the geometry is exactly the same as the molybdenum NSTAR grids. For the PG grids, due to fabrication limitations, the screen grid is 17% thicker and all other dimensions are the same.

A genetic search algorithm was used to identify new candidate geometries and these new grid geometries were evaluated using 2D and 3D ion optics codes developed at JPL. There are six parameters that determine the grid geometry as listed in Table 2. This list of parameters defines the ion optics characteristics for a single pair of screen and accelerator grid apertures. For a complete grid set two additional geometric parameters are needed: the dish depth and the amount of compensation of the accelerator grid hole spacing to account for the hole misalignment due to dishing.

Table 2. Grid Geometry Parameters.

Parameter	Symbol
Screen Grid Hole Diameter	d_s
Screen Grid Thickness	t_s
Accelerator Grid Hole Diameter	d_a
Accelerator Grid Thickness	t_a
Center-to-Center Hole Spacing	l_{cc}
Grid Gap	l_g

The service life of the accelerator grid is limited by erosion of the grid apertures and erosion of the "pits & grooves" pattern on the downstream surface of the grids. The 3D code was used to investigate the dependence of the pit & grooves erosion geometry on the grid geometry. This investigation indicated that the following parameters have little impact on the shape of the pits and grooves erosion pattern: center-to-center hole spacing, accelerator hole diameter, discharge chamber plasma density, and screen grid thickness.

The 2D code was used to evaluate the perveance, electron-backstreaming, and accelerator hole wall erosion rates for the candidate grid designs. This investigation indicated that the accelerator grid life based on hole wall erosion is solely a function of the beamlet current density extracted and the electric field and, to first order, is not a function of the grid geometry. Therefore, the grid geometry is selected to maximize the mechanical robustness of the screen grid while meeting the perveance and screen grid transparency requirements.

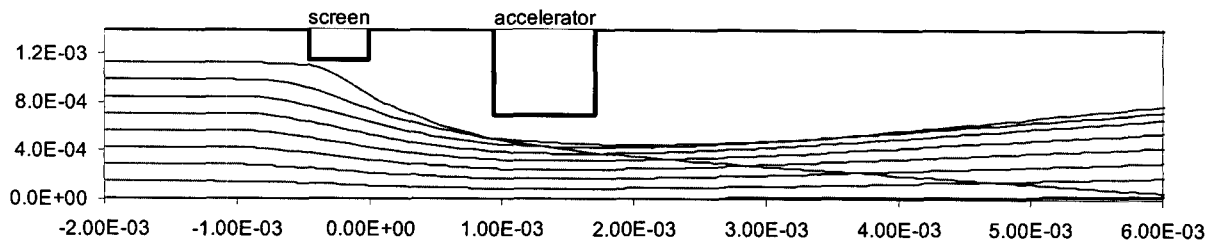


Fig. 2. Calculated Ion Trajectories for Carbon-Carbon Grid Design for Operation at 4000 sec.

The perveance and screen grid transparency are most strongly functions of the intra-grid electric field. The perveance is also a function of the screen and accelerator hole diameters and thicknesses. The screen grid transparency is a strong function of the screen grid open area fraction and the screen grid thickness.

Maximizing the perveance and screen grid transparency require maximizing the intra-grid electric field. Maximizing the grid separation to prevent grid-to-grid contact during vibration testing while minimizing the potential for grid-to-grid arcing requires minimizing the intra-grid electric field. The selected grid design uses the minimum electric field that enables the design to meet the perveance and screen grid transparency requirements. This minimum electric field is approximately 2300 V/mm and results in a grid gap of 0.93 mm for operation with at a specific impulse of 4000 s. A plot of the ion trajectories through the grid apertures calculated using the 2D code is given in Fig. 2. Two variations on this design are being fabricated in CC. One has a screen grid open area fraction of 67% and the other 70%.

In addition to the modeling work performed at JPL, experimental studies of optics designs are being performed at Colorado State University with "gridlets," small, flat, carbon coupons made of grid material with only some tens of apertures. Perveance and crossover measurements are made in an effort to correlate gridlet behavior to full-scale grid behavior and also to study the effects of the number of gridlet apertures, increased accelerator grid hole size (to simulate a grid set that has been operating for an extended time) and grid spacing (to simulate a non-uniform grid gap) on the optics performance. A complete discussion of this work is provided in Ref. 14.

Carbon-Carbon Structural Design

The structural design of the CBIO carbon-carbon grids implements lessons learned during previous development efforts. The major fabrication problem with the last published development effort, for example, was the loss of control of the grid radius of curvature.¹ Other issues included poor flatness of the mounting ring structure and slightly non-spherical grid shapes.

Each of these can lead to poor grid gap control and aperture alignment. Curvature control and grid sphericity have been addressed in the CBIO carbon-carbon grids through design and process control, and verified by inspection (discussed in a subsequent section). A double-walled cylinder mounting and support ring, shown in Fig. 3, has been designed for better control of flatness and surface parallelism compared to earlier designs. This new design also incorporates a greater stiffness, light weight and ease of manufacturing.

A stiffening ring has been added to the accelerator grid as well. This ring, seen on the periphery of the grid in the full optics assembly view of Fig. 4, is primarily used to increase the stiffness and flatness of the accelerator grid.

A major concern in design of the CC grids is that they must survive the launch vibration loads while meeting the performance requirements set out in Table 1. A previous CC grid set developed by JPL¹ fractured during vibration testing and it is believed that the fracture was caused by grid-to-grid contact during

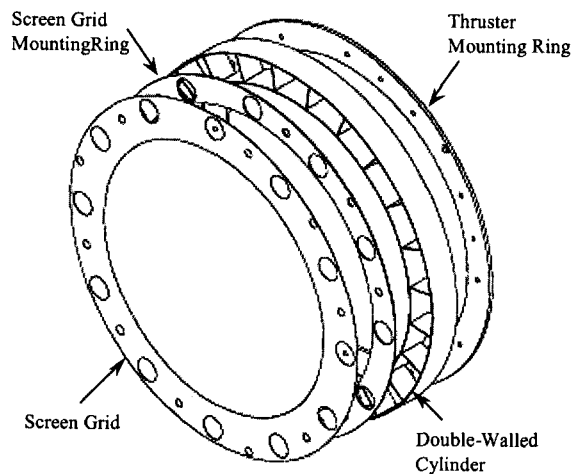


Fig. 3. Exploded View of CBIO Carbon-Carbon Screen Grid Assembly.



Fig. 4. CBIO Carbon-Carbon Optics Assembly.

the test. Hence, a primary objective of the CBIO structural design is to avoid contact between the grids. The increased stiffness and dish depth of the grids and mounting structure design will help reduce grid deflection during vibration testing. The goal of eliminating grid-to-grid contact is considered conservative because the thicker MUSES-C grids survived vibration testing even with grid-to-grid contact.⁵

Preliminary dynamic modeling has proven the benefits of increased dish depth for a sample grid geometry. Model calculations of the screen grid assembly first natural frequency as a function of dish depth are shown in Fig. 5 along with the sum of the 3- σ displacements for both accelerator and screen grids. Increasing the dish depth clearly increases the stiffness

of the structure and reduces the probability of grid impact during vibration testing. Although this analysis was not performed for the exact geometry of the grids that fractured during vibration, it can be seen that the small dish depth of that grid set (5 mm) was probably insufficient to prevent grid-to-grid contact at typical ion thruster grid gaps (~0.6 mm). It was thus decided that larger dish depths should be incorporated in the CBIO grid design. A dish depth of 23 mm was eventually selected, based on many design considerations.

Carbon-Carbon Fabrication

Fabrication of the CC grids follows a similar process to that described in Refs. 1 and 2, using a layup of the $[0^\circ/+60^\circ/-60^\circ]$ type. Unidirectional P-30X fiber tape is layed over graphite molds, placed in a vacuum bag to form the layup shape, then cured at a modest temperature. A carbonization step follows, then the material is densified with a chemical vapor infiltration process. Heat treatment is used to stiffen the materials. The grids are laser machined to produce the apertures and assembly features, then bonded to the stiffening rings. The screen grid is additionally bonded to the double-walled cylinder. A final chemical vapor deposition (CVD) process is used to give the assemblies a finishing carbon coat.

As mentioned previously, control of the grid radius of curvature was a major issue during an earlier development.¹ In that work, the finished grids had a curvature that was different than the design value by 10-15%. This resulted in a grid set that could not be assembled and operated in the traditional outwardly-dished manner. Because the curvature was only

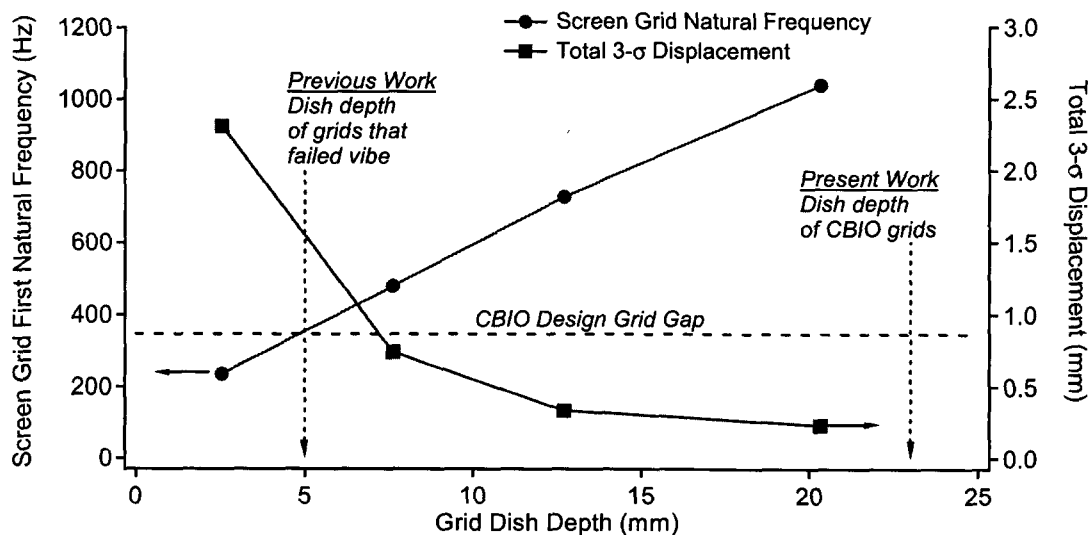


Fig. 5. Predicted Carbon-Carbon Grid Dynamic Response.

measured for the final parts, it was not known which process of the fabrication caused the most change. Hence, in order to understand the causes of the curvature change, a batch of four grid sets constructed before the initiation of the CBIO program with the same materials and processes (hereafter referred to as the "pre-CBIO" grids) was carefully studied during fabrication.

The radius of curvature of the four pre-CBIO grid sets, nominally 57 cm, was measured at several points between fabrication steps. Results of the curvature measurements for accelerator grid #3 are shown in Table 2. Note that the 56.85-cm curvature before heat treatment was measured after the layup, cure, graphitization, and densification steps. It is evident that the newer materials and processes yield net curvature changes that are significantly less than the 10-15% seen in Ref. 1. The majority of the change that did occur was during the heat treatment step.

Table 2. Radius of Curvature Measurements for Accelerator Grid #3.

Grid Measurement	Radius of Curvature (cm)	Percent Change From Previous Step
Tooling – Concave	57.35	—
Tooling – Convex	56.45	—
Before Heat Treat	56.85	—
After Heat Treat	57.72	1.55%
After Aperture Machining	57.74	0.02%
Final Grid	58.00	0.45%

Table 3 compares the relative curvature changes due to the heat treatment and laser machining processes for grid sets #1 and #3. Similar results are seen for both grid sets, indicating the degree of process repeatability. The radius of curvature of the screen grids changed by a lesser amount than did the accelerator grids. It is not known if this was caused by the different grid blank thicknesses or because the screen and accelerator grids were heat treated together inside the same tooling set. The accelerator grids had almost no curvature change due to the aperture machining; unfortunately the coordinate measurement machine (CMM) probe used to measure the grid curvatures caused excessive deflection of the thin, machined screen grids and the data were not considered useable (non-contact inspection methods are now being used to measure the radius of curvature of these parts).

Grid sets #2 and #4 were processed in a different order than that described above. For these, the

Table 3. Radius of Curvature Change During Processing of Carbon-Carbon Grids.

Grid Set #	Change due to heat treatment		Change due to aperture machining	
	Accelerator	Screen	Accelerator	Screen
1	1.22%	0.57%	0.02%	*
3	1.55%	0.66%	0.02%	*

* CMM measurement caused part deflection, which rendered results unusable.

apertures were laser machined before the heat treatment step. Inspection of the grids showed that curvature change during the heat treatment was sufficient to cause aperture misalignment, thus those grids are unusable and the original fabrication procedure is preferred. The tooling for the CBIO grid layups was designed to account for the curvature change observed during the heat treatment process shown in Table 2 so that the final curvatures of the accelerator and screen grids will be identical. Additionally, the screen and accelerator grids are heat treated in their own individual tooling to better control the curvature.

The sphericity of the completed grids was also a concern in an earlier work¹ so characterization of the pre-CBIO grids was performed. Accelerator grid #3 was inspected with the CMM after final processing and the Cartesian data from the dished surface were fit to a sphere. Two separate measurements yielded a radius of curvature of 58.00 cm with standard deviations from a perfect spherical shape of only 0.03 mm (i.e. less than 4% of the design grid gap).

Pyrolytic Graphite Design

Similar concerns to the CC ones are present and are addressed in the fabrication of the PG grids. This is done by carefully designing the optics assembly mounting structure and maintaining close involvement with the grid vendors to ensure a good understanding of the design parameters that influence their processes and machining operations. Some of these parameters include maintaining critical dimensions such as hole diameters, dish depth, and hole concentricities. To maintain design geometries and voltage standoff parameters in the active region of the PG grids during operation, Boeing EDD has designed an optics assembly holding fixture based on a pin and groove methodology. This design allows the grids to expand and contract radially while still maintaining aperture concentricity and appropriate grid separation. Titanium stiffening rings were chosen to match as closely as possible the thermal expansion properties of the grids.

As with CC, a major concern is the response of the PG material to vibrational loads. Although final results are not yet complete, initial computer modeling results show that the combined dish depth, grid thicknesses, optics assembly holding fixture, and stiffening rings are

sufficiently designed to prevent the grids from contacting during vibration at NSTAR levels. The vibration test of the PG grids on an NSTAR engineering model thruster is expected to be completed in July 2003.

Pyrolytic Graphite Fabrication

Pyrolytic graphite is formed through a pyrolysis reaction, which is basically the chemical vapor deposition (CVD) of carbon. Free carbon atoms deposit on a mandrel, layer after layer, thus taking on its shape. Atomic bonds are strong in the plane parallel to the mandrel surface (the A-B plane) and much weaker in the growth direction (the C direction). Hence, materials properties are significantly different in the C direction compared to those in the A-B plane. For example, although the in-plane strength of PG is good, the weaker interlayer bonds in the C-direction make PG susceptible to delamination if shearing stresses are present.

The pyrolytic graphite used in the CBIO program is manufactured by Minteq International of Easton, Pennsylvania. The grade of pyrolytic graphite used is a hybrid of their "Continuously Nucleated" and their "Substrate Nucleated." The hybrid provides more desirable properties for ion thruster grids than either material by itself.

The PG grids are grown on high-purity-grade graphite mandrels where they take on the desired geometry. This is done to avoid cutting through planes of graphite during the machining phase, which may lead to a decrease in structural rigidity, delamination, and compromise of the in-plane anisotropic properties that make PG a good choice for grid material. Instead, the grids are grown oversize so that they can be machined to final thickness of which there is greater control in holding dimensional tolerances. Therefore, cutting through planes is minimized as the cut follows the contours of the planes. Once they are machined to the correct thickness, they are heat treated at roughly 200 °C higher than the deposition temperature to relieve stresses induced by the machining. The result is a grid blank that is of the desired shape and thickness, and is ready for the 15,000-plus apertures which are mechanically drilled. Shown in Fig. 6 is a completed PG optics assembly.

TEST ACTIVITIES

Performance Testing - Flat Carbon-Carbon Grids

Preliminary work at JPL on the CBIO project involved building a power-supply rack and data acquisition and command system that could operate at the required thruster operating parameters, specifically at the higher required beam voltages. This system was first tested with an available set of flat 30-cm CC grids



Fig. 6. Pyrolytic Graphite Optics Assembly.

produced as a part of the pre-CBIO activity. This particular grid set, designed for operation at Isp's of 4000-5000 sec, had the hole pattern shown in Table 4 and a grid gap of 1.4 mm. Unfortunately, these grids were fabricated before process controls were well-developed and the hole alignment was thus imperfect. Performance testing was performed on the JPL-built NSTAR-Knock-Off (NKO) thruster that is similar in design and performance to the NSTAR thruster.

Table 4. Flat Carbon-Carbon Grid Hole Pattern.

	Screen	Accelerator
Hole Diameter (mm)	4.159	2.418
Open Area Fraction	0.71	0.24
Grid Thickness (mm)	0.75	1.00

These flat CC grids were operated over a variety of test conditions and at Isp's up to 5300 secs – the highest Isp ever demonstrated on carbon-based thruster grids. The capabilities of the grids and test equipment were verified at beam voltages of up to 3000 V, intra-grid electric fields of up to 2500 V/mm, and beam currents of up to 1.8 A. Over eighteen hours of operation were accumulated with these grids at beam voltages greater than 1500 V. While there was relatively frequent arcing during the first few tens of minutes of grid operation, the rate of arcing decreased considerably after initial testing and did not adversely affect thruster operation and test activities. Similar initial arcing has been seen in many other CC grid tests.

Perveance, electron backstreaming, and screen grid transparency measurements were made with the flat CC grids operating at screen and accelerator grid voltages of 2900 V and -450 V, respectively. Perveance measurements were made by holding the beam current constant while varying the screen grid voltage and recording the accelerator grid current. The discharge current was adjusted in this case to maintain the constant beam current. Electron backstreaming (EBS)

onset was determined by lowering the accelerator grid voltage and monitoring the beam ion energy cost. The screen grid transparency was measured by biasing the screen grid negative of the cathode by twenty volts and recording the bias current. The ratio of the screen power supply current to the total screen current (i.e. bias current plus screen supply current) yields the transparency.

Perveance and electron backstreaming results are shown in Figs. 7 and 8, respectively, for three beam currents. These results are provided in summary with the other measurement results in Table 5 for the operating conditions investigated. It can be seen that this grid set provides significant backstreaming margin for all operating conditions and adequate perveance margin for all but the highest beam current case. The screen grid transparency is higher than 75% for all but the 1.76-A beam current case. Poorer performance at the higher beam current test conditions was likely aggravated by the imperfect aperture alignment of this grid set.

Vibration Testing

Vibration testing of the 30-cm dished pre-CBIO grids was performed in order to validate the model predictions for grid dynamic response. There was also uncertainty in some of the materials properties of the finished CC composite grids, so vibration testing offered an opportunity to gather more information and adjust the models accordingly.

Testing was performed at Boeing EDD using a random vibration spectrum that was similar to an early NSTAR protoflight specification¹⁵ but with higher RMS vibration levels. The accelerator and screen grid assemblies were vibrated separately in order to preclude grid-to-grid contact during the model validation portion of the testing. Both grid assemblies were instrumented with accelerometers on the active grid area as well as strain gauges on the grid periphery.

The accelerator grid assembly was tested first. Although originally of the pre-CBIO design, a stiffening ring was bonded to the accelerator grid to make the structure identical to the final CBIO design. After a preliminary sine sweep to measure the assembly

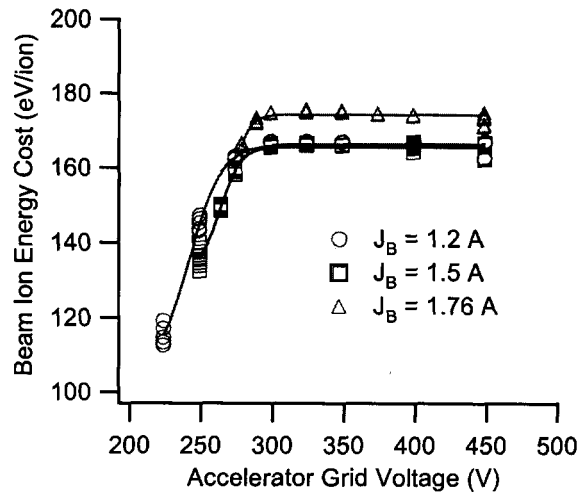


Fig. 7. Perveance Measurements for Flat Carbon-Carbon Grids.

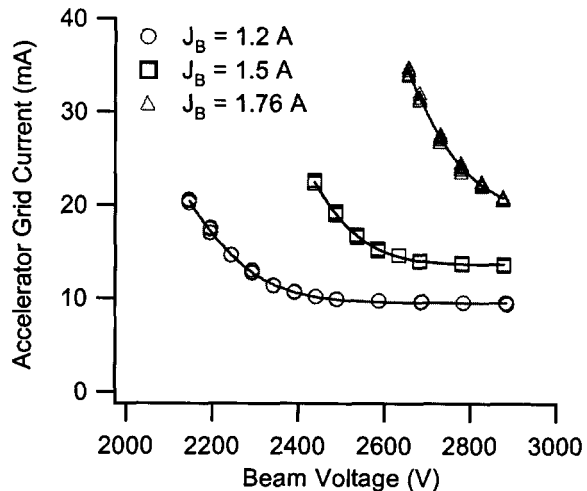


Fig. 8. Electron Backstreaming Measurements for Flat Carbon-Carbon Grids.

Table 5. Performance of Flat Carbon-Carbon Optics at a Total Voltage of 3350 V.

Throttle Level	Beam Current (A)	Calculated Isp (sec)	Perveance Limit (V)	Perveance Margin (V)	EBS Limit (V)	EBS Margin (V)	Screen Transparency
0	0.51	4120	1310	1590	275	175	0.894
3	0.61	4520	1490	1410	250	200	0.882
6	0.91	4937	1950	950	250	200	0.850
9	1.20	5135	2350	550	275	175	0.801
12	1.49	5093	2600	300	275	175	0.769
15	1.76	4977	2900	0	280	170	0.734

natural frequencies, total random vibration RMS loads were slowly incremented up to the full load of 18.6 Grms (roughly double the NSTAR random vibration qualification test load). Low-level load response data were acquired immediately before and after the full-load test and compared to ensure grid integrity. The accelerator grid assembly survived the full-load random vibration test with no visible damage and no tell-tale frequency shifts in the pre- and post-test low-level load responses.

The vibration test data were then analyzed and compared to the pre-test predictions. In the process, the material modulus and the damping coefficient for the first vibrational mode were adjusted to provide better correlation with test results. After these adjustments, the model predicted natural frequencies that were very close to the measured data as seen in Table 6. Table 7 shows that good correlation with the accelerometer measurements during the random vibration test was also achieved, with the exception of #5. The reason for the discrepancy is unknown at this time, but could be due to poor accelerometer adhesion to the grid during the test (difficulties with accelerometer adhesion affected the measured responses during preliminary testing of the screen grid assembly).

Table 6. Comparison of measured and predicted accelerator grid natural frequencies.

Natural Frequency	Calculation	Measurement	Difference
1st	859.0 Hz	840 Hz	-2.3%
2nd	1055.5 Hz	1024 Hz	-3.1%
3rd	1055.5 Hz	-	-
4th	1364.0 Hz	1428 Hz	4.5%
5th	1364.8 Hz	-	-

A comparison of the measured and predicted power spectral density response of accelerometer #1, located on the grid centerline, is shown in Fig. 9. Agreement up to and including the first natural frequency is excellent. Better correlation for the higher natural frequencies is likely with adjustment of the modal damping coefficients, but this effort has not yet begun. Adjustment of the higher damping coefficients, however, would not add substantially to the overall

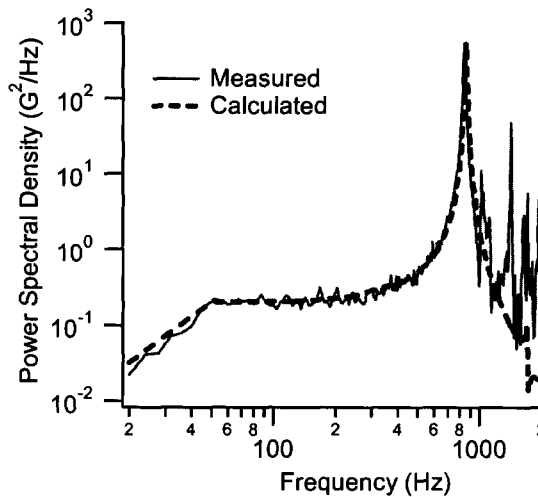


Fig. 9. Comparison of Measured and Calculated Response to 18.6 Grms Stimulation at Accelerator Grid Centerline.

calculated response shown in Table 7. The calculated RMS displacement for the curve in Fig. 9 is 0.04 mm, less than 5% of the CBIO design grid gap.

Preliminary screen grid assembly vibration tests have also been performed and analysis of the results is underway. Following correlation of the test data and calculations, the full grid set will be assembled and subjected to the same vibration tests.

Voltage Standoff and Arcing

A series of tests were performed on the voltage standoff capability and damage to the CC material due to induced arcing. The experimental set up consisted of a classic vacuum "plate and ball" configuration, where flat samples of CC grid material without apertures were spaced a given distance in a vacuum system from a 2.5 cm-diameter graphite ball at ground potential. The system was evacuated to pressures of at least the 10^{-6} Torr range, then the CC sample was biased negatively relative to the ball and the threshold voltage at which significant field emission occurred was measured as a function of the separation distance between the two electrodes. Electrical breakdown between the electrodes was then triggered by over-volting the gap with a high voltage pulser, which

Table 7. Comparison of measured and predicted accelerator grid responses at 18.6 Grms stimulation.

Accelerometer	Location		Calculation	Measurement	Difference
	Radius	Angle			
1	0 mm	0°	123.2 G's	129.0 G's	4.7%
2	21 mm	180°	122.7 G's	129.8 G's	5.5%
3	64 mm	180°	108.9 G's	107.5 G's	-1.3%
4	102 mm	180°	117.2 G's	124.7 G's	6.0%
5	102 mm	90°	117.2 G's	199.6 G's	70.3%

discharged a capacitor through a current-limiting resistor into the arc between the electrodes.

The threshold for field emission, defined arbitrarily in these experiments by the voltage (or electric field) at which 1 μA of current was drawn between the electrodes, was measured as a function of the gap between the ball and plate. The as-manufactured CC material demonstrated a remarkable ability to hold voltage, with a threshold electric field of 12 to 15 kV/mm at electrode spacings of 0.25 mm.

The sample was then connected to the negative leg of the pulser, and a series of ten arcs were forced. The arc current was detected by a current transformer and the data stored by a digital oscilloscope that automatically integrated the current pulse to provide the total charge transfer for each pulse.

The threshold electrode field was measured after each of the arc events for various values of the system capacitance and series resistance. An example of these data is shown in Fig. 10 for the case of 0.25-mm spacing and 5-kV charging voltage. The field emission threshold data are shown for two capacitances and three different values for the series current-limiting resistance in the circuit.

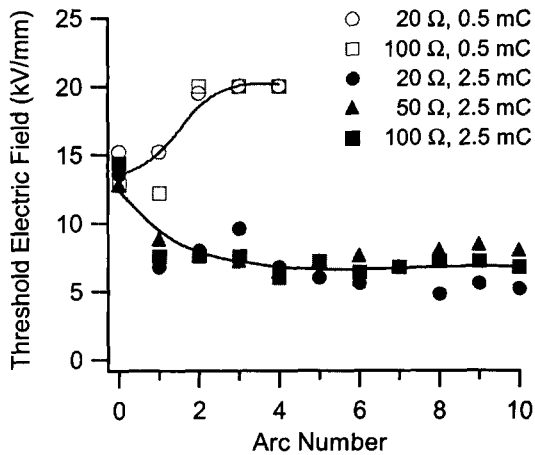


Fig. 10. Arc Effects on Carbon-Carbon Voltage Standoff Capability.

It can be seen that for charge transfers of 0.5 C, the threshold electric field actually increased indicating conditioning of the surface had occurred. In this case, the CC material withheld electric fields characteristic of carefully smoothed and cleaned high voltage electrode surfaces made of materials such as copper and molybdenum. Visual inspection of the surface under a microscope showed that the surface had been nicely smoothed by the arcing, which improved the voltage hold off capability. However, for the case of 2.5 mC of charge transfer, the field emission threshold degraded by about a factor of two by the arcing. Visual

inspection of the surface showed considerable roughening in the region of the arcing.

The data also show that the size of the series resistor in the circuit does not change the surface damage and threshold for field emission. While series resistance is normally introduced into power supply circuits to limit fault currents, it does not change the amount of energy deposited in the surface or change the amount of material removed that results in roughening of the surface and degradation of the voltage hold off. Proper design of the power supply to suppress or eliminate grid damage during arcing requires limiting the total coulomb transfer in the arc event. This is normally done by limiting the amount of stored energy in the power supply, or providing series or parallel switching in the output to limit the energy delivered to a fault.

Finally, it should be noted that although these charge transfer levels roughened the surface and degraded the voltage hold off, the CC composite material still demonstrated the ability to hold off high electric fields before significant field emission occurred. In this case, the "damaged" surface withstood electric fields of over 5 kV/mm across a 0.25 mm gap with leakage currents of only 1 μA . In reality, to induce an arc the voltage had to be increased significantly and the field emission exceed tens of microamps before arcing actually occurred. It is clear that if the fault current transfer can be minimized, CC composite material can hold the electric fields of interest for ion thruster grids.

Sputter Yield Measurements

An understanding of the sputter yields of both PG and CC materials is necessary for grid life modeling and calculations. In addition to the total yield (atoms/ion), the differential yield (atoms/ion/steradian) must be obtained in order to accurately assess the effects of redeposition of sputtered material. Measurements of both total and differential yield for the PG and CC materials used in the CBIO project are being performed at Colorado State University.

Sputter yield measurements were performed by directing a 2.5-cm-dia. xenon ion beam onto the center of the target located 23 cm away. The target could be rotated with respect to the ion beam to investigate incidence angles of 0° to 70°. Deposition of sputtered material was detected by a quartz crystal microbalance (QCM) located 17.8 cm from the target. The QCM could be rotated within a single plane at angles of -90° to +90° with respect to the target normal for differential yield measurements. Further description of the facilities and methods is given in Ref. 16.

Sputter yields of PG material were measured first at xenon ion energies of 300 to 1000 eV. Differential yield data for PG at an ion energy of 1 keV are shown

in Fig. 11 for several incidence angles. In this figure, the ion beam is directed toward the target from the negative angles (i.e. the left-hand side of the plot) at the incidence angles indicated next to the individual traces. The total sputter yield for the normal incidence data in the figure is obtained by integrating the differential yield and is 0.26 atoms/ion. Total yields for the non-normal incidence angles can be calculated if an assumption is made about the behavior of the differential yield outside of the measurement plane¹⁶ (differential yields over the entire hemisphere were not obtained for this study).

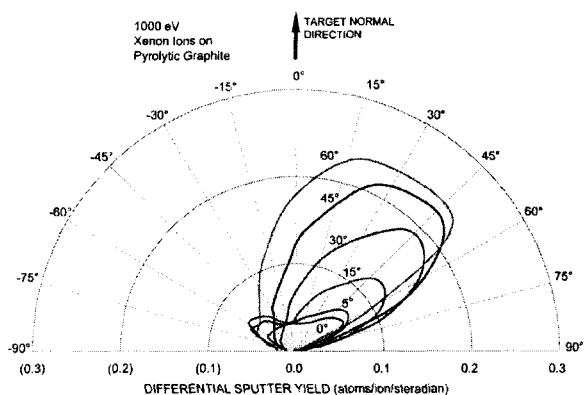


Fig. 11. Differential Sputter Yield Data for 1-keV Xenon Ions on Pyrolytic Graphite Over a Range of Incidence Angles.

FUTURE ACTIVITIES

Performance testing of the CBIO grids will be performed at JPL and Boeing EDD on NSTAR-like thrusters. In addition to the optics performance measurements, Faraday probes will be used to characterize beam divergence and an ExB probe will be used to measure the double-ion content of the beam. After vibration testing, the performance characterization tests will be repeated.

Several criteria will be used to evaluate and compare the PG and CC grids in the downselect process. An endurance test of the selected grid technology will then be conducted at JPL. The goals of the test are to (1) demonstrate 2000 hours of operation of the carbon grids on a 30-cm diameter NSTAR-like thruster at a beam current of 1.76 A and a beam voltage of 1800 V, and (2) demonstrate erosion rates on the accelerator grid at least a factor of three less than molybdenum for the same peak beam current density and grid voltages.

Successful conclusion of the Phase I portion of the CBIO project will support the Phase II efforts. The Phase II objectives are to design and fabricate 40-cm

diameter carbon grids for the NEXT thruster, characterize the performance of the grids on the NEXT thruster, and perform an endurance test on the NEXT thruster of at least 2000 hours. An additional objective will be to evaluate the mission benefits of carbon grids for NASA's family of ion thrusters.

CONCLUSIONS

Carbon-carbon and pyrolytic graphite ion optics have been designed and fabricated for 4000-sec operation and performance requirements derived from the NEXT requirements. The CC grids have been manufactured with significantly improved process control compared to earlier CC development efforts. The PG and CC grids have been designed to maximize mechanical robustness and the CC structural design was verified by successful grid vibration tests at levels up to 18.6 Grms with no signs of grid damage. Computer dynamic models of grid response during vibration testing were shown to accurately predict the response of the CC grids, validating these dynamic models as accurate design tools for grid sets with different hole patterns and larger diameters.

A series of experiments was performed that examined the voltage standoff capabilities of PG and CC and the behavior of the materials after arc damage was induced. Carbon-carbon was shown to stand off electric fields of up to 20 kV/mm and could stand off fields of 5 kV/mm after "damage" was induced. Fundamental understanding of the voltage standoff behavior of the PG and CC materials is being obtained which will enable the design of laboratory and flight power supplies to reduce the risk of arc damage to carbon grid materials to acceptable levels.

Performance and vibration testing of the PG and CC grids developed under the CBIO program will be performed beginning in July 2003. The results of those tests will be used to select a technology, which will be subjected to the 2000-hour endurance test. Grid life and performance modeling, supported by differential sputter yield measurements and gridlet test activities, will be used to predict the results of the upcoming 2000-hour endurance test of PG or CC grids.

Successful completion of Phase I of the CBIO program is expected to lead to the Phase II work in which 40-cm carbon grids will be manufactured. These grids, after performance and vibration testing, will be subjected to an endurance test on the NEXT thruster.

ACKNOWLEDGEMENTS

The authors would like to thank Dr. Wei Shih of Allcomp, Inc., for fabrication of the carbon-carbon grids for JPL. The authors would also like to acknowledge the contributions of Dr. Brian Sullivan

and the team at Materials Research & Design, Inc., for the vibration models and analyses. Mark Johnson, a Graduate Research Assistant in the Mechanical Engineering Department at Colorado State University, performed the sputter measurements. Thanks to Drs. Keith Goodfellow and Dennis Fitzgerald of JPL for design and setup of the high-voltage test equipment and data acquisition and control system, and to Mr. Allison Owens and Mr. Ray Swindlehurst of JPL for fabrication and assembly of test and facility hardware.

This research was carried out, in part, at the Jet Propulsion Laboratory, California Institute of Technology, under a contract with the National Aeronautics and Space Administration. Funding was provided by the In-Space Transportation Program managed by Les Johnson at the NASA Marshall Space Flight Center. The CBIO program is managed by Randy Baggett. Their support is gratefully acknowledged.

REFERENCES

1. J. Mueller, J.R. Brophy, and D.K. Brown, "Design, Fabrication, and Testing of 30-cm Dia. Dished Carbon-Carbon Ion Engine Grids," AIAA 96-3204, 32nd Joint Propulsion Conference, Lake Buena Vista, FL, July 1996.
2. J. Mueller, J.R. Brophy, and D.K. Brown, "Endurance Testing and Fabrication of Advanced 15-cm and 30-cm Carbon-Carbon Composite Grids," AIAA 95-2660, 31st Joint Propulsion Conference, San Diego, CA, July 1995.
3. J. Mueller, J.R. Brophy, D.K. Brown, and C.E. Garner, "Performance Characterization of 15-cm Carbon-Carbon Composite Grids," AIAA 94-3118, 30th Joint Propulsion Conference, Indianapolis, IN, June 1994.
4. D.E. Hedges and J.S. Meserole, "Demonstration and Evaluation of Carbon-Carbon Ion Optics," J. of Propulsion and Power, Vol. 10, No. 2, March-April 1994, pps. 255-261.
5. I. Funaki, H. Kuninaka, K. Toki, Y. Shimizu, K. Nishiyama, and Y. Horiuchi, "Verification Tests of Carbon-Carbon Composite Grids for Microwave Discharge Ion Thruster," J. of Propulsion and Power, Vol. 18, No. 1, Jan-Feb 2002, pps. 169-175.
6. Y. Hayakawa, S. Kitamura, and K. Miyazaki, "Endurance Test of C/C Grids for 14-cm Xenon Ion Thrusters," AIAA 2002-3958, 38th Joint Propulsion Conference, Indianapolis, IN, July 2002.
7. H. Kuninaka, S. Satori, Y. Horiuchi, "Continuous Operation Test of Microwave Discharge Ion Thruster System," AIAA 95-3070, 31st Joint Propulsion Conference, San Diego, CA, July 1995.
8. S. Kitamura, K. Miyazaki, Y. Hayakawa, Y. Nakamura, and S. Yamaguchi, "Fabrication and Testing of Carbon-Carbon Composite Grids for a 14-cm Ion Thruster," IEPC 95-93, 24th International Electric Propulsion Conference, Moscow, Russia, 1995.
9. T. Haag and G. Soulas, "Performance of 8-cm Pyrolytic-Graphite Ion Thruster Optics," AIAA 2002-4335, 38th Joint Propulsion Conference, Indianapolis, IN, July 2002.
10. J.R. Anderson, J.E. Polk, and J.R. Brophy, "Service Life Assessment for Ion Engines," IEPC 97-049, 25th International Electric Propulsion Conference, Cleveland, OH, 1997.
11. Patterson, M.J., Foster, J.E., Haag, T.W., Rawlin, V.K., Soulas, G.C., and R.F. Roman, "NEXT: NASA's Evolutionary Xenon Thruster," AIAA 2002-3832, 38th Joint Propulsion Conference, Indianapolis, IN, July 2002.
12. D. Rosenberg, and G.K. Wehner, "Sputtering Yields for Low Energy He⁺, Kr⁺, and Xe⁺ Ion Bombardment," J. Applied Physics, V. 33, n. 5, May 1962, pp. 1842-1845.
13. R. Deltschew, M. Tartz, V. Plicht, E. Hartmann, H. Neumann, H.J. Leiter, and J. Esch, "Sputter Characteristics of Carbon-Carbon compound Material," IEPC 01-118, 27th International Electric Propulsion Conference, Pasadena, CA, Oct. 2001.
14. D.M. Laufer, J.D. Williams, and P.J. Wilbur, "Experimental Evaluation of Sub-Scale CBIO Ion Optics Systems," AIAA 2003-5165, to be presented at the 39th Joint Propulsion Conference, Huntsville, AL, July 2003.
15. J.S. Sovey et al., "Development of an Ion Thruster and Power Processor For New Millennium's Deep Space 1 Mission," AIAA 97-2778, 33rd Joint Propulsion Conference, Seattle, WA, July 1997.
16. J.D. Williams, M.M. Gardner, M.L. Johnson, and P.J. Wilbur, "Xenon Sputter Yield Measurements for Ion Thruster Materials," IEPC 03-130, 28th International Electric Propulsion Conference, Toulouse, France, March 2003.